An algebraic geometric method for calculating phase equilibria from fundamental equations of state

Hythem Sidky,[1] Alan C. Liddell, Jr,[2] Dhagash Mehta,[1,2] Jonathan D. Hauenstein,[2,a)] and Jonathan Whitmer[1,b)]

[1)] *Department of Chemical and Biomolecular Engineering, University of Notre Dame, Notre Dame, IN 46556, USA.*

[2)] *Department of Applied and Computational Mathematics and Statistics, University of Notre Dame, Notre Dame, IN 46556, USA.*

Computing saturation properties from highly–accurate Helmholtz equations of state can be challenging for many reasons. The presence of multiple Maxwell loops often results in incorrect solutions to equations defining fluid phase coexistence. Near the critical point, the same equations also become ill–conditioned. As a consequence, without highly accurate initial guesses, it is difficult to avoid the trivial solution. Here, we propose an algorithm applying the technique of Newton homotopy continuation to determine the coexistence curve for all vapor–liquid equilibrium conditions between the triple point and critical point. Importantly, our algorithm is entirely convergence–parameter free, does not rely on the use of auxiliary equations, requires no initial guesses, and can be used arbitrarily close to the critical point. It is also fully generalizable to arbitrary equations of state, only requiring that they be locally analytic away from the critical point. We demonstrate that the method is capable of handling both technical and reference quality fundamental equations of state, is computationally inexpensive, and is useful in both evaluating individual state points and plotting entire fluid phase envelopes.

Keywords: phase equilibrium, saturation conditions, Newton homotopy, phase equilibrium, nonlinear equations, numerical algebraic geometry

I. INTRODUCTION

The modern fundamental equation of state (FEOS) represents the state-of-the-art in high accuracy thermodynamic property description of fluids. These equations of state are typically explicit in Helmholtz free energy as a function of temperature and density, allowing for all thermodynamic quantities of interest to be expressed through combinations of partial derivatives and equality constraints. The ability of FEOS to represent properties within the error of the most accurate experimental data[1] has driven the development of publicly available software[2,3] supplanting the use of traditional printed tables.

FEOS can be broadly classified into two categories[4], with *reference equations of state* offering superior reliability, extrapolation behavior, and lower uncertainty, particularly near the critical point. The functional forms are often fluid specific and contain a significant number of terms, incorporate non-analytic expressions and as a consequence, have been developed for only a handful of fluids including water[5], carbon dioxide[6], nitrogen[7], argon[8], methane[9], ethane[10], propane[11], ethylene[12] and sulfur hexaflouride[13]. In contrast, *technical equations of state* are available for a much wider range of fluids, often sharing simultaneously optimized forms across entire fluid classes[14–17]. The requirements on experimental data are less stringent with the resulting equations containing exclusively analytic and far fewer terms.

Due to the explicit Helmholtz energy form, single phase thermodynamic quantities such as pressure, fugacity, enthalpy, heat capacity and other common coefficients can be calculated directly at fixed temperature and density by taking the appropriate partial derivatives. On the other hand, in the two–phase region, the equilibrium densities at a fixed temperature must first be identified using an iterative method, after which the desired properties can be computed. This can prove to be challenging as FEOS often present multiple solutions at low temperatures and a narrow binodal with poor numerical conditioning near the critical point. To address these issues, auxiliary equations are fit to saturation data during the development of the initial FEOS and used as a source of high-quality initial guesses. Furthermore, a combination of algorithmic and heuristic approaches assist in convergence and identifying the correct solutions.

As an alternative to the use of successive substitution and classical Newton–Raphson (NR), which are common but require the use of auxiliary equations, Akasaka[18] proposed a damped NR scheme. In the method, a convergence parameter γ which dampens the Newton step is adjusted after each iteration. The algorithm's stability is enhanced and converges successfully without the use of auxiliary equations at low to moderate temperatures. However, near the critical point the use of a new starting guess is required. The temperature at which the starting guess is switched depends on the fluid and can range from a few degrees K to nearly $50\,\mathrm{K}$[18] away from the critical point. Such an approach requires tabulation of limiting temperatures and is not convenient for maintaining an up–to–date database of fluid equations. Also, despite being more robust, this method fails within the immediate vicinity of the critical point ($\approx 0.1\,\mathrm{K}$) due to poor conditioning of the Jacobian[3]. Span[1] utilized the Regula

a)Electronic mail: hauenstein@nd.edu
b)Electronic mail: jwhitme1@nd.edu

Falsi method, a derivative–free bracketed root finding algorithm, to solve the saturation equations for both pure fluids[1] and multicomponent mixtures[19]. While it overcomes some difficulties associated with poor conditioning, the rate of convergence is linear and a search interval must be known *a priori*[20]. This method also proves to be challenging near the critical point as the two phase region becomes exceptionally narrow.

In this work we use numerical algebraic geometry (NAG) to develop a *convergence–parameter free* method for determining the saturation states of FEOS. NAG techniques, including various forms of homotopy continuation, have previously been applied to a variety of thermodynamic problems[21–23] including phase stability analysis of cubic equations of state[24] and critical point determination.[25,26] The algorithm we propose here is generalizable to arbitrary EOS models as will be described below, but is specifically adapted and tested on Helmholtz–explicit FEOS. It uses no auxiliary equations and relies exclusively on the analytic properties of the system of equations away from the critical point to reliably determine the equilibrium conditions. The use of adaptive multi–precision homotopy continuation[27] allows the algorithm to robustly obtain solutions arbitrarily close to the critical point where the objective function may be ill–conditioned and even non–analytic. Furthermore, utilizing temperature as a natural homotopy parameter such as this one enables the tracing of the entire binodal and spinodal curves between the triple and critical points in an efficient manner, using predictor–corrector steps to guide sampling along the path.

II. THE PROBLEM SET UP

The modern Helmholtz–explicit FEOS is generally formulated as the sum of the non–dimensionalized ideal ($\alpha^0(\tau, \delta)$) and residual ($\alpha^r(\tau, \delta)$) Helmholtz energy[1]:

$$\frac{a(T, \rho)}{RT} = \alpha(\tau, \delta) = \alpha^0(\tau, \delta) + \alpha^r(\tau, \delta) \quad (1)$$

where a is the specific Helmholtz free energy, R is the gas constant, T is the temperature, and ρ is the density. The independent variables τ and δ are the inverse reduced temperature and reduced density respectively. Given the Helmholtz free energy, all thermodynamic properties in the single phase can be obtained through appropriate derivatives of α. For example, the isochoric heat capacity can be defined as

$$\frac{c_v}{R} = \tau^2 \left(\frac{\partial^2 \alpha}{\partial \tau^2} \right)_\delta. \quad (2)$$

The ideal gas contribution α^0 is usually defined via correlations of the heat capacity or the Helmholtz free energy directly. The general formulation of the residual term, determined through a complex optimization pro-

cedure, can be written as[1]

$$\alpha^r(\tau, \delta) = \sum n_i \tau^{t_i} \delta^{d_i} + \sum n_i \tau^{t_i} \delta^{d_i} \exp(-\gamma_i \delta^{p_i})$$
$$+ \sum n_i \tau^{t_i} \delta^{d_i} \exp\left(-\eta_i(\delta - \varepsilon_i)^2 - \beta_i(\tau - \gamma_i)^2\right) \quad (3)$$
$$+ \sum n_i \delta \Delta^{b_i} \exp\left(-e_i(\delta - 1)^2 - f_i(\tau - 1)^2\right)$$

where

$$\Delta = \left\{ (1 - \tau) + c_i \left[(\delta - 1)^2\right]^{1/(2\beta_i)} \right\}^2 + d_i \left[(\delta - 1)^2\right]^{a_i}. \quad (4)$$

The first two summations are common and found across both technical and reference equations of state. The Gaussian summation improves accuracy in the critical region and the final summation is non-analytic and captures the true behavior of the isochoric heat capacity and speed of sound within the immediate vicinity of the critical region. Variables with the subscript i represent parameters that are determined during the fitting process and can be specific to an individual fluid or a class of substances.

The equilibrium of the liquid phase ($'$) and vapor phase ($''$) at a given temperature T_s, independent of the specific functional form of the equation of state, satisfies the following conditions:

$$p(\rho', T_s) = p(\rho'', T_s) \quad (5)$$
$$g(\rho', T_s) = g(\rho'', T_s) \quad (6)$$

where g is the Gibbs free energy and p is the unknown saturation pressure. Using the simple density dependence of α^0 and recognizing that

$$\frac{p}{\rho RT} = 1 + \delta \alpha_\delta^r \quad (7)$$

and

$$\frac{g}{RT} = 1 + \alpha^0 + \alpha^r + \delta \alpha_\delta^r \quad (8)$$

allows for the conditions to be rewritten as

$$\delta'(1 + \delta' \alpha^r(\tau, \delta')) = \delta''(1 + \delta'' \alpha^r(\tau, \delta'')) \quad (9)$$

and

$$\delta' \alpha_\delta^r(\tau, \delta') + \alpha_\delta^r(\tau, \delta') + \ln \delta' = \delta'' \alpha_\delta^r(\tau, \delta'') + \alpha_\delta^r(\tau, \delta'') + \ln \delta''. \quad (10)$$

We note that the two simultaneous equations (9) and (10) are implicit in pressure and have no explicit dependence on the ideal gas free energy α^0. With ρ' and ρ'' as the two unknowns, the novel algorithm developed to solve these equations is described below. The obtained densities are then substituted back into (7) to determine pressure, or any other derived thermodynamic identity.

III. NEWTON HOMOTOPY

A core part of the algorithm involves the use of homotopy continuation applied to a Newton homotopy to obtain solutions of a system of nonlinear equations. Mathematically speaking, a *homotopy* is a continuous deformation of one continuous function into another. That is, given two functions f, g with domain X and target Y, a homotopy $H : X \times [0,1] \to Y$ is a continuous function on $X \times [0,1]$ such that $H(x,0) = f(x)$ and $H(x,1) = g(x)$. Numerical algebraic geometry uses *homotopy continuation* to solve systems of nonlinear equations. By casting a target system f as a member of a family of systems containing another system g, one whose solutions are known or readily found, we may continuously deform g into f. The solutions of $H(x,t) = 0$ describe one or more one-real-dimensional curves, called *paths* which start at solutions of $g = 0$ and end at solutions of $f = 0$.

The responsibility of numerical algebraic geometry is tracking these paths, which entails producing a sequence of numerical approximations to points along these curves, starting at $t = 1$ and terminating at $t = 0$. Numerical homotopy continuation uses predictor-corrector methods to compute these approximations, such as an Euler predictor and a Newton corrector, though higher-order predictors, such as classical Runge–Kutta and its variants, are used in practice. These methods are implemented in the software package `Bertini`[28,29], utilized in this work, which also makes use of adaptive step sizes, adaptive precision[27], and especially *endgames*[30] (see discussion below) to handle the various difficulties that come with numerically tracking paths, namely regions of ill-conditioning in the vicinity of the critical point.

Broadly, an endgame is an algorithm which approximates a (possibly singular) solution to $H(x,0)$ given points along the path. Provided that the solution paths defined by $H(x,t)$ are smooth on $(0,1]$ and that the system $H(x,t)$ itself is locally analytic for all $t \in (0,1]$, we may track each solution path from $t = 1$ to $t = 0$. Near $t = 0$, the tracking will employ various endgames to handle singular solutions to $H(x,0) = f(x) = 0$. Switching from a path tracking algorithm to an endgame algorithm is often necessary because, in the ill-conditioned regions near singularities, pressing on with path tracking can be prohibitively expensive in terms of precision and step size.

We will employ Newton homotopies to force solutions together and to see where they meet. A linear homotopy between f and g has the form

$$H(x;t) = (1 - t) \cdot f(x) + t \cdot g(x).$$

A *Newton homotopy* is a homotopy in which only the constant terms depend on t. In the context of a linear homotopy, this means that $f(x) - g(x)$ is constant, say $v = f(x) - g(x)$. A Newton homotopy has the form

$$H(x;t) = f(x) - t \cdot v.$$

Suppose that $f(x;p) = 0$ is a system of equations where x is a variable and p is a parameter. For a fixed parameter p_0, suppose further that x_0 and y_0 are two distinct solutions of $f(x;p_0) = 0$. We may wish to determine how to vary the parameter p in order for the two distinct solution paths starting at x_0 and y_0, respectively, to meet at a single solution z^* corresponding to some new parameter p^*. Using a Newton homotopy, one may now consider p as a variable and consider the homotopy:

$$H(x,y,p;t) := \begin{bmatrix} f(x,p) \\ f(y,p) \\ x - y \end{bmatrix} - t \cdot \begin{bmatrix} 0 \\ 0 \\ x_0 - y_0 \end{bmatrix}.$$

The point (x_0, y_0, p_0) is clearly a solution to the system $H(x,y,p;1) = 0$. If the solution path through this point is smooth on $(0,1]$, then, as t approaches 0, the two distinct solutions y_0 and z_0 corresponding to parameter p_0 will be forced to merge into a single solution z^* corresponding to a new parameter p^*. This observation is the key to our algorithm.

IV. ALGORITHM

The first step in solving the saturation equations is identifying the appropriate spinodals, corresponding to the points where $(\partial p / \partial \rho)_T = 0$ which are used in subsequent steps. Due to the lack of constraints on the FEOS between the spinodals, most exhibit undesirable behavior in the unstable two phase region. This often gives rise to multiple Maxwell loops which are problematic for numerical solvers because they produce additional unphysical solutions. For our purposes, the equations can present additional points satisfying the saturation conditions. To illustrate this phenomenon, Figure 1 compares the pressure–density isotherms for n-butane at $300\,\text{K}$ using the Peng–Robinson EOS, the original Benedict–Webb–Rubin (BWR) EOS[31] and the technical FEOS by Span and Wagner[15]. The FEOS shows a prominent oscillation while the BWR EOS has a subtle secondary convexity at low density. In contrast, the classical PR–EOS shows a single physical Maxwell loop which is characteristic of cubic equations of state.

Near the critical point, the narrowness of the binodal only complicates matters further. It becomes challenging to obtain a non-trivial solution without the use of high quality starting guesses. Lemmon and Jacobsen[32] developed a new functional form that yields only one solution for phase equilibrium at a given state, not unlike cubic EOS, through the addition of certain nonlinear fitting constraints. However, many existing FEOS do not make use this functional form and its application to reference type FEOS remains limited.

In our method, we take advantage of the fact that the outermost stationary points $\partial P / \partial \rho = 0$ always correspond to the true limits of stability[1]. These outermost vapor and liquid spinodals can be determined easily and
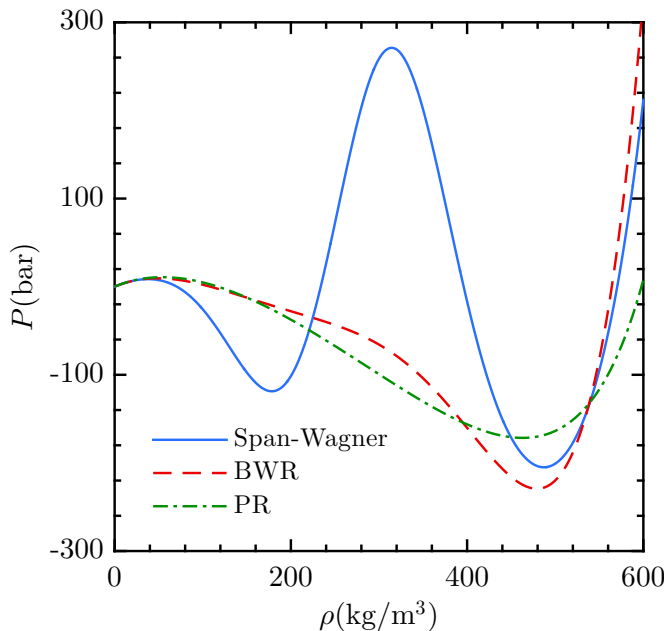
Figure 1. P–ρ isotherm at $300\,\mathrm{K}$ for n-butane showing both the metastable and unstable regions using the Span–Wagner technical fundamental equation of state[15] (solid line), Benedict–Webb–Rubin (BWR) equation of state[31] (dashed line) and Peng–Robinson (PR) equation of state (dash-dotted line). Both the BWR and FEOS exhibit additional Maxwell loops which give rise to unphysical solutions.

Algorithm 1: Algorithm for computing spinodals

input : Initial temperature T_0, boundary density ρ_0
output: Spinodal density ρ_s that satisfies
$\left.\frac{\partial P}{\partial \rho}\right|_{T=T_0,\,\rho=\rho_s} = 0$

---

1. Compute $\left.\frac{\partial P}{\partial \rho}\right|_{T=T_0,\,\rho=\rho_0}$ and store in dP_0

2. Construct $H(\rho;t) := \left.\frac{\partial P}{\partial \rho}\right|_{T=T_0} - t \cdot dP_0$

3. Evolve the homotopy from $t = 1$ to $t = 0$ and store result in ρ_s

---

reliably by "rolling downhill" or "climbing uphill" respectively. Any reasonable choice of univariate root finding algorithm is sufficient for solving $(\partial P/\partial \rho)_{T=T_0} = 0$ and is initialized by approaching $P(\rho;T)$ from 0 and ∞, which, in practice, is a very large number. We utilize a Newton homotopy formulated in Algorithm 1 for both 0 and ∞. This step is usually performed at a low temperature, typically near or at the triple point, as there is significant separation between the liquid–like and vapor-like densities.

After computing the spinodals, we present two variants of the algorithm for obtaining either a solution to the saturation equations at a particular state condition, or alternatively an entire phase diagram for the fluid.

In our first approach, at or near the triple point, we use the spinodals as starting guesses to compute the vapor and liquid densities. This data can be used as the start-

ing point for tracking to a particular temperature using the Newton homotopy defined in Algorithm 2. Rather than tracking to a particular temperature, Algorithm 3 tracks the binodals until the vapor and liquid densities are equal. The advantage of this algorithm is that an endgame can be used to accurately compute the ending data using data collected along the path potentially far away from the ill-conditioned region near the critical point.

Algorithm 2: Algorithm for tracking binodals to a particular temperature

input : Start temperature T_0, starting densities ρ_{liq}, ρ_{vap} satisfying
$\begin{bmatrix} P(\rho_{liq}, T_0) \\ g(\rho_{liq}, T_0) \end{bmatrix} = \begin{bmatrix} P(\rho_{vap}, T_0) \\ g(\rho_{vap}, T_0) \end{bmatrix}$, and target temperature T^*.
output: Densities ρ_{liq}^*, ρ_{vap}^* that satisfies
$\begin{bmatrix} P(\rho_{liq}^*, T^*) \\ g(\rho_{liq}^*, T^*) \end{bmatrix} = \begin{bmatrix} P(\rho_{vap}^*, T^*) \\ g(\rho_{vap}^*, T^*) \end{bmatrix}$

---

1. Construct a homotopy consisting of Eqns. (9) and (10), with temperature T as a variable such that
$H(\rho_l, \rho_v, T; t) := \begin{bmatrix} P(\rho_l, T) - P(\rho_v, T) \\ g(\rho_l, T) - g(\rho_v, T) \\ T - T^* - t(T_0 - T^*) \end{bmatrix}$
2. Evolve the homotopy from $t = 1$ to $t = 0$ and store the results in ρ_l^*, ρ_v^*, T_{end}.
if $T_{end} = T^*$ **then**
  return $\rho_{liq}^* := \rho_l^*$, $\rho_{vap}^* := \rho_v^*$
else
  return failure
end

The second approach uses a two-step approach which is summarized in Figure 2. The first step tracks the entire spinodal curve using the algorithm in Section 4 starting from the spinodal data computed above at low temperature. In this algorithm, the spinodal densities are tracked as a function of temperature until the critical point is reached, at which point the critical temperature and density is returned. Since the binodal and spinodal curves intersect at the critical point, the final state of the spinodal homotopy is also a solution to (9) and (10). At this intersection point, one can use a local tangent cone computation[33] to yield the first prediction along the binodal curve after which a predictor-corrector tracking employed on the Newton homotopy in Section 2 can be used to track down to the low temperature point.

These procedures are not expensive and require only a handful of function evaluations for must use cases, as detailed below. Both approaches are equally reliable under certain conditions and discussed in the results. For all homotopies, tracking is performed using the adaptive step–size Runge–Kutta–Fehlberg (RKF45) predictor–corrector method with multi–precision arithmetic and the power series endgame[29,30]. This enables

Algorithm 3: Algorithm for tracking binodals to convergence

input : Start temperature T_0, starting densities ρ_{liq}, ρ_{vap} satisfying
$$\begin{bmatrix} P(\rho_{liq}, T_0) \\ g(\rho_{liq}, T_0) \end{bmatrix} = \begin{bmatrix} P(\rho_{vap}, T_0) \\ g(\rho_{vap}, T_0) \end{bmatrix}$$

output: Critical temperature T_c and density ρ_c satisfying $\begin{bmatrix} \partial P / \partial \rho|_{\rho=\rho_c} \\ \partial g / \partial \rho|_{\rho=\rho_c} \end{bmatrix} = 0$

---

1. Construct a homotopy consisting of Eqns. (9) and (10), with the density difference $\rho_l - \rho_l$ as a variable such that

$$H(\rho_l, \rho_v, T; t) := \begin{bmatrix} P(\rho_l, T) - P(\rho_v, T) \\ g(\rho_l, T) - g(\rho_v, T) \\ \rho_l - \rho_v - t(\rho_{liq} - \rho_{vap}) \end{bmatrix}$$

2. Evolve the homotopy from $t = 1$ to $t = 0$ and store the results in ρ_l^*, ρ_v^*, T^*

if $\rho_l^* = \rho_v^*$ **then**
  | **return** $\rho_c := \rho_l^*$, $T_c := T^*$
else
  | **return** failure
end

Algorithm 4: Algorithm for tracking spinodals to convergence

input : Start temperature T_0, spinodal densities ρ_{liq} and ρ_{vap} with $\rho_{liq} \neq \rho_{vap}$

output: Critical temperature T_c, density ρ_c, satisfying $\frac{\partial P}{\partial \rho}\big|_{T=T_c, \, \rho=\rho_c} = 0$

---

1. Construct a homotopy to determine to determine the stationary points of P with respect to $\rho_{v,l}$ such that $H(\rho_l, \rho_v, T; t) := \begin{bmatrix} \frac{\partial P}{\partial \rho}\big|_{\rho=\rho 1} \\ \frac{\partial P}{\partial \rho}\big|_{\rho=\rho 2} \\ \rho_l - \rho_v - t \cdot (\rho_{liq}^* - \rho_{vap}^*) \end{bmatrix}$

2. Evolve the homotopy from $t = 1$ to $t = 0$ and store the results in ρ_l^*, ρ_v^*, T^*

if $\rho_l^* = \rho_v^*$ **then**
  | **return** $\rho_c := \rho_l^*$, $T_c := T^*$
else
  | **return** failure
end

the solver to compute data arbitrarily close to the critical point even with functional forms such as those for CO_2[6] and water[5] since the homotopy only requires the system to be locally analytic.

It is important to note that although the procedures may seem redundant, as the critical point of a fluid is known beforehand, it is a required step for a truly *convergence–parameter free* method. Technical fundamental equations of state such as those of Span and Wagner[14] are not constrained to the supplied critical parameters. Thus, in order to avoid the use of tabulated *resulting* critical parameters, they can be determined as such, and applicable to all equations of state. The resulting T_c, ρ_c of the fluid are then used to initiate the binodal tracking.

V. RESULTS

The newly developed method is applied to the technical FEOS for nonpolar and weakly polar fluids[14,15] and reference FEOS for CO_2[6] developed by Span and Wagner. The functional form of α^r for the former FEOS is

$$\begin{aligned}
\alpha^r(\delta, \tau) = & \, n_1 \delta \tau^{0.25} + n_2 \delta \tau^{1.125} + n_3 \delta \tau^{1.5} + n_4 \delta^2 \tau^{1.375} \\
& + n_5 \delta^3 \tau^{0.25} + n_6 \delta^7 \tau^{0.875} + n_7 \delta^2 \tau^{0.625} e^{-\delta} \\
& + n_8 \delta^5 \tau^{1.75} e^{-\delta} + n_9 \delta \tau^{3.625} e^{-\delta^2} + n_{10} \delta^4 \tau^{3.625} e^{-\delta^2} \\
& + n_{11} \delta^3 \tau^{14.5} e^{-\delta^3} + n_{12} \delta^4 \tau^{12.0} e^{-\delta^3},
\end{aligned}$$
$$(11)$$

where the parameters n_i are fluid specific. This functional form and its polar fluid counterpart[16] have been applied to a broader selection of fluids[17] and are representative of many similar[34–38] fluid specific equations.
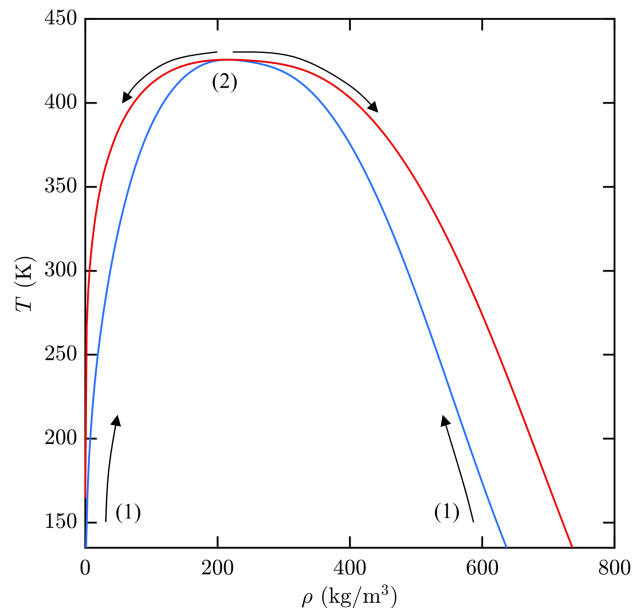
Figure 2. Temperature–density spinodals and binodals for n–butane using the Span–Wagner technical FEOS[14,15] highlighting the novel algorithm where (1) the spinodal is tracked from the triple point to the critical point, then (2) the binodals are tracked back down to the triple point.

We first demonstrate the complete mapping of the vapor-liquid phase diagram for n–butane using the proposed algorithm. Figure 2 shows the two–step homotopy process and the resulting diagram. First, the spinodals at the triple point (134.9 K) are determined using Algorithm 1 by locating the outermost stationary points at fixed temperature. Using Algorithm 4, the spinodal den-

Table I. Critical properties evaluated from the Span–Wagner technical FEOS[15] for nonpolar and weakly polar fluids.

Substance	T_c (K)	P_c (MPa)	ρ_c (kg/m^3)
Methane	190.6123	4.6057	159.969
Ethane	305.5093	4.8871	196.798
Propane	369.9388	4.2554	213.325
n–Butane	425.7588	3.8303	215.473
n–Pentane	469.6590	3.3688	235.199
n–Hexane	507.7945	3.0416	222.825
n–Heptane	541.2259	2.7738	224.901
n–Octane	569.5704	2.5066	227.626
Argon	150.7914	4.8798	520.530
Oxygen	154.7087	5.0616	419.861
Nitrogen	126.2535	3.4045	307.348
Ethylene	282.4544	5.0504	206.281
Isobutane	407.7495	3.6331	217.280
Cyclohexane	553.6511	3.9836	262.889
SF$_6$	318.7239	3.7544	718.886

Figure 3. Saturation curves for nonpolar and weakly polar fluids[15] obtained using the novel algorithm described in this work.

sities are then tracked to the critical temperature. Once the critical density and temperature are known, the values are used to initiate tracking of the binodal curves following Algorithm 2 back down to the triple point. The result is the entire coexistence curve for the fluid. We emphasize that outside the fluid-specific parameters for α^r, no additional information was required.

A good measure of the accuracy for the proposed method is a comparison of the evaluated critical properties to those reported in the original work[15]. As previously mentioned, this technical FEOS was not constrained to exactly represent the critical point of the fluids, as doing so would require additional terms to fulfill requirements outside the extended critical region[14]. Thus, the critical values used to reduce temperature and density for a given fluid do not correspond to the same critical values admitted by the FEOS. Table I shows the evaluated critical properties using our method for all fluids in the original work. With the exception of a single fluid, all numbers match those in Ref. 15 identically to numerical precision. The discrepancy is only in ρ_c for argon and lies in the second–least significant digit. There are a number of potential reasons for this, one of which may be the use of higher precision in our calculations; we report our values to an additional significant digit for reference. Figure 3 shows the reduced saturation curves for all fluids described by the technical FEOS.

Next, we evaluate the performance and robustness of this method on the Span–Wagner CO_2 FEOS[6] that contains a non-analytic term Δ in (4) which results in a divergence of the heat capacity at the critical point. It is preferable to adopt the alternative procedure described in Section IV. The reason for this is illustrated in Figure 4. In the neighborhood of the critical point, the liquid–phase spinodal curve which was tracked from the triple point, exhibits a jump discontinuity. At ≈ 303.8985 K,
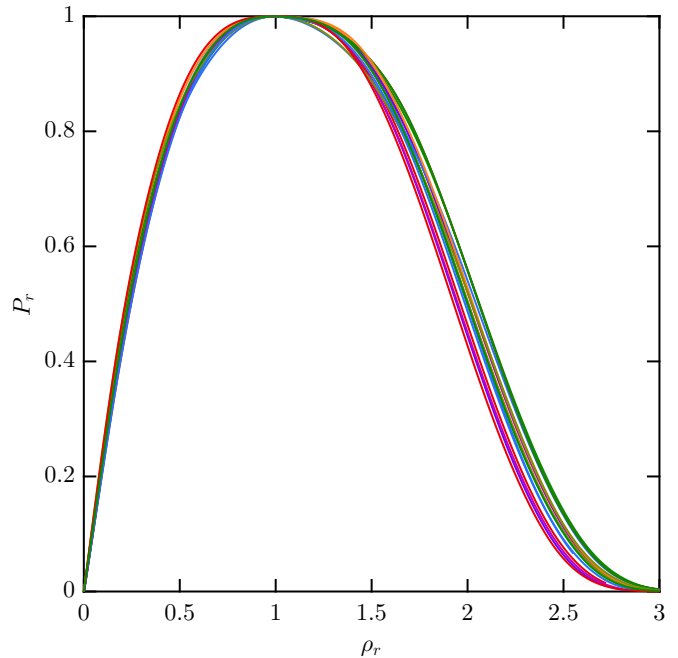
the identity of the "outermost" stationary point, and effectively the Maxwell loop, changes to an interior point which was previously beyond the limit of mechanical stability. The cause of this phenomenon can be understood by looking at $\partial P/\partial \rho$ for temperatures near the discontinuity as shown in Figure 5. With increasing temperature, there is an upwards shift in $\partial P/\partial \rho$ until the outermost stationary point becomes an inflection point. It is doubtful that this discontinuity was intended to capture physical behavior, as there exists little experimental data this far into the metastable region. More likely is that the Gaussian damping associated with the non–analytic term for the critical region causes this artifact. This nonetheless highlights additional considerations that may be im-
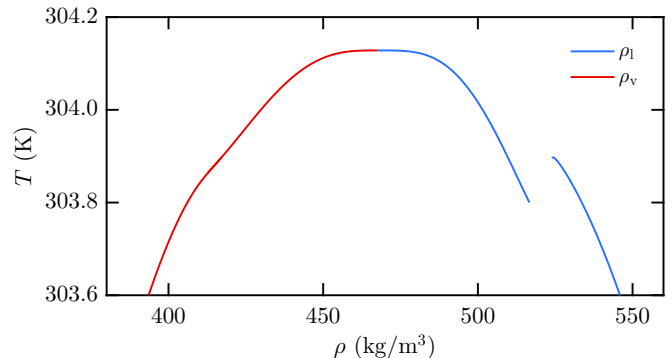

Figure 4. Spinodal curves near the critical point for CO_2 described by the Span–Wagner FEOS[6] showing a jump discontinuity in the "exterior" liquid–phase spinodal.

portant when developing new functional forms for fluids.

The jump discontinuity observed for CO_2 can present difficulties when tracking the spinodal curves to the critical point using Algorithm 4. However, using the alternative procedure, Algorithm 3, completely avoids this issue. It is important to emphasize that the previous scheme is equally valid for systems without jumps in the spinodals, and is quite useful for plotting the entire saturation curve. The following approach is well suited for solving the saturation equations user–specific conditions and for plotting the entire binodal. Firstly, as with the previous method, the spinodals at the triple point are identified using Algorithm 1. The spinodal densities are then used as the start system for a homotopy to solve the saturation equations (9) and (10). Once the saturated densities are determined, the binodals are tracked to a pre–specified condition using Algorithm 2. Figure 6 (a) shows the result of tracking the saturation curve from the triple point to the critical point. The open circles indicate the points at which the equations were evaluated. Only 17 evaluations are required to reach a temperature of 303 K, which is comparable to the damped Newton method proposed by Akasaka[18]. However, unlike the damped Newton method which fails to converge at temperatures above 303 K, our approach is able to get arbitrarily close to the critical point. This comes at the expense of function evaluations, which as shown in Figure 6(b), approaches 80 to get within 10^{-7} of T_c with 10 digits of precision on the densities. It is unlikely that most scientific applications require such a degree of precision, yet it is still possible using this method. Fewer evaluations are needed to achieve equivalent tolerances for the technical FEOS due to better conditioning near the critical point.
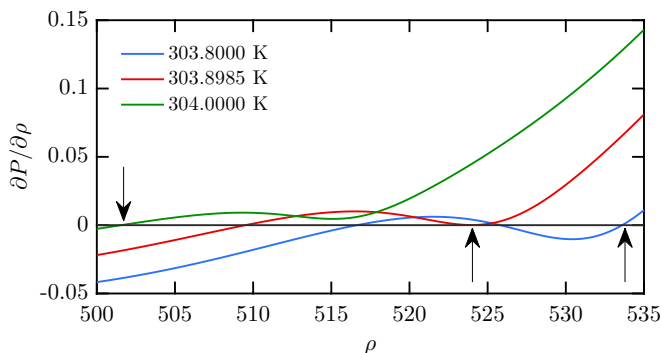

Figure 5. Density derivative of pressure for CO_2 described by the Span–Wagner FEOS[6]. Note the precise temperature at which the outermost stationary point changes identity. The arrows point to the outermost stationary point at various temperatures.

VI. CONCLUSION

We present an algebraic geometric method based on homotopy continuation applied to Newton homotopies to robustly determine saturation conditions for Helmholtz–explicit fundamental equations of state. The proposed algorithm does not rely on the use of auxiliary equations or initial guesses and is entirely parameter–free. Adaptive step–sizes and precision allow the reliable evaluation of saturation properties along the entire saturation curve, and in particular within the immediate vicinity of the critical point. Two variants of the algorithm are described in order to deal with potential discontinuities in the spinodal curves, which can be used to map the entire phase diagram.

Though demonstrated for particular equations of state, this approach is fully general and should work with any locally analytic model. Extensions of this method are possible to multicomponent mixtures where it becomes more challenging to identify the appropriate densities. Utilizing this method in computer applications can greatly increase the robustness of density–solvers near the critical point where the trivial solution is difficult to escape, and eliminates the need for auxiliary equations.

REFERENCES

[1] R. Span. *Multiparameter Equations of State.* Springer Berlin Heidelberg, Berlin, Heidelberg, 2000.

[2] E.W. Lemmon, M.L. Huber, and M.O. McLinden. NIST Standard Reference Database 23: Reference Fluid Thermodynamic and Transport Properties-REFPROP, 2013.

[3] I.H. Bell, J. Wronski, S. Quoilin, and V. Lemort. Pure and Pseudo-pure Fluid Thermophysical Property Evaluation and the Open-Source Thermophysical Property Library CoolProp. *Industrial & Engineering Chemistry Research*, 53(6):2498–2508, feb 2014.

[4] R. Span, W. Wagner, E.W. Lemmon, and R.T. Jacobsen. Multiparameter equations of state recent trends and future challenges. *Fluid Phase Equilibria*, 183-184:1–20, 2001.

[5] W. Wagner and A. Pruß. The IAPWS formulation 1995 for the thermodynamic properties of ordinary water substance for general and scientific use. *Journal of Physical and Chemical Reference Data*, 31(2):387–535, 2002.

[6] R. Span and W. Wagner. A New Equation of State for Carbon Dioxide Covering the Fluid Region from the Triple-Point Temperature to 1100 K at Pressures up to 800 MPa. *Journal of Physical and Chemical Reference Data*, 25(6):1509, 1996.

[7] R. Span, E. W. Lemmon, R. T. Jacobsen, W. Wagner, and A. Yokozeki. A Reference Equation of State for the Thermodynamic Properties of Nitrogen for Temperatures from 63 . 151 to 1000 K and Pressures to 2200 MPa. *Journal of Physical Chemistry Reference Data*, 29(6), 2001.

[8] C. Tegeler, R. Span, and W. Wagner. A New Equation of State for Argon Covering the Fluid Region for Temperatures From the Melting Line to 700 K at Pressures up to 1000 MPa. *Journal of Physical and Chemical Reference Data*, 28(3):779, 1999.

[9] U. Setzmann and W. Wagner. A New Equation of State and Tables of Thermodynamic Properties for Methane Covering the Range from the Melting Line to 625 K at Pressures up to 100 MPa. *Journal of Physical and Chemical Reference Data*, 20(6):1061–1155, 1991.

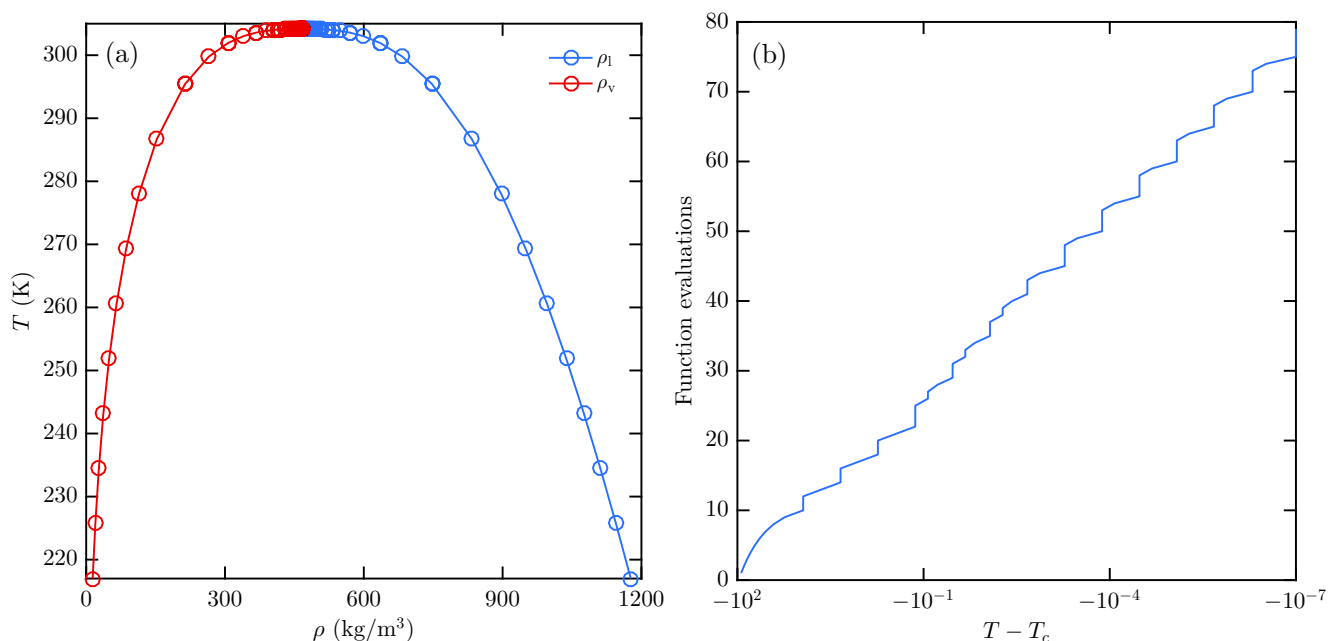[10] D. Bücker and W. Wagner. A reference equation of state for the

Figure 6. Complete saturation curve for CO_2 described by the Span–Wagner FEOS[6] obtained by Newton homotopy tracking of the binodal densities. The points at which the equations are evaluated are shown (a) on the diagram as open circles. The increase in the number of function evaluations required to achieve a final tolerance of 10^{-7} at various temperatures approaching the critical point (b) are also plotted.

thermodynamic properties of ethane for temperatures from the melting line to 675 K and pressures up to 900 MPa. *Journal of Physical and Chemical Reference Data*, 35(1):205–266, 2006.

[11]E.W. Lemmon, M.O. McLinden, and W. Wagner. Thermodynamic properties of propane. III. A reference equation of state for temperatures from the melting line to 650 K and pressures up to 1000 MPa. *Journal of Chemical and Engineering Data*, 54:3141–3180, 2009.

[12]J. Smukala, R. Span, and W. Wagner. New Equation of State for Ethylene Covering the Fluid Region for Temperatures From the Melting Line to 450 K at Pressures up to 300 MPa. *Journal of Physical and Chemical Reference Data*, 29(5):1053, sep 2000.

[13]C. Guder and W. Wagner. A reference equation of state for the thermodynamic properties of sulfur hexafluoride (SF6) for temperatures from the melting line to 625 K and pressures up to 150 MPa. *Journal of Physical and Chemical Reference Data*, 38(1):33–94, 2009.

[14]R. Span and W. Wagner. Equations of State for Technical Applications. I. Simultaneously Optimized Functional Forms for Nonpolar and Polar Fluids. *International Journal of Thermophysics*, 24(1):1–39, 2003.

[15]R. Span and W. Wagner. Equations of State for Technical Applications. II. Results for Nonpolar Fluids. *International Journal of Thermophysics*, 24(1):41–109, 2003.

[16]R. Span and W. Wagner. Equations of State for Technical Applications. III. Results for Polar Fluids. *International Journal of Thermophysics*, 24(1):111–162, 2003.

[17]E.W. Lemmon and R. Span. Short Fundamental Equations of State for 20 Industrial Fluids. *Journal of Chemical & Engineering Data*, 51(3):785–850, may 2006.

[18]R. Akasaka. A Reliable and Useful Method to Determine the Saturation State from Helmholtz Energy Equations of State. *Journal of Thermal Science and Technology*, 3(3):442–451, 2008.

[19]J. Gernert, A. Jäger, and R. Span. Calculation of phase equilibria for multi-component mixtures using highly accurate Helmholtz energy equations of state. *Fluid Phase Equilibria*, 375:209–218, 2014.

[20]W.H. Press, S.A. Teukolsky, W.T. Vetterling, and B.P. Flannery. *Numerical Recipes 3rd Edition: The Art of Scientific Computing*. Cambridge University Press, New York, NY, USA, 3 edition, 2007.

[21]J. Bausa and W. Marquardt. Quick and reliable phase stability test in VLLE flash calculations by homotopy continuation. *Computers & Chemical Engineering*, 24(11):2447–2456, 2000.

[22]I. Malinen, J. Kangas, and J. Tanskanen. A new Newton homotopy based method for the robust determination of all the stationary points of the tangent plane distance function. *Chemical Engineering Science*, 84:266–275, 2012.

[23]H. Zhang. A review on global optimization methods for phase equilibrium modeling and calculations. *The Open Thermodynamics Journal*, 5(1):71–92, 2011.

[24]A.C. Sun and W.D. Seider. Homotopy-continuation method for stability analysis in the global minimization of the Gibbs free energy. *Fluid Phase Equilibria*, 103(2):213–249, 1995.

[25]M.C. Wang, D.S.H. Wong, H. Chen, W. Yan, and T.-M. Guo. Homotopy continuation method for calculating critical loci of binary mixtures. *Chemical Engineering Science*, 54(17):3873–3883, 1999.

[26]H. Sidky, D. Mehta, and J. Whitmer. Reliable mixture critical point computation using polynomial homotopy continuation. *AIChE Journal*, 2016.

[27]D.J. Bates, J.D. Hauenstein, A.J. Sommese, and C.W. Wampler. Adaptive multiprecision path tracking. *SIAM Journal on Numerical Analysis*, 46(2):722–746, 2008.

[28]D.J. Bates, J.D. Hauenstein, A.J. Sommese, and C.W. Wampler. Bertini: Software for numerical algebraic geometry (2006). *Software available at http://bertini. nd. edu.*

[29]D.J. Bates, J.D. Hauenstein, A.J. Sommese, and C.W. Wampler. Numerically solving polynomial systems with Bertini. 25:xx+352, 2013.

[30]A.J. Sommese and C.W. Wampler. *The Numerical solution of systems of polynomials arising in engineering and science*, vol-

ume 99. World Scientific, 2005.

[31] M. Benedict, G.B. Webb, and L.C. Rubin. An Empirical Equation for Thermodynamic Properties of Light Hydrocarbons and Their Mixtures I. Methane, Ethane, Propane and n-Butane. *The Journal of Chemical Physics*, 8(4):334–345, 1940.

[32] E.W. Lemmon and R.T. Jacobsen. A New Functional Form and New Fitting Techniques for Equations of State with Application to Pentafluoroethane (HFC-125). *Journal of Physical and Chemical Reference Data*, 34(1):69, 2005.

[33] W. Hao, J.D. Hauenstein, B. Hu, Y. Liu, A.J. Sommese, and Y.-T. Zhang. Continuation along bifurcation branches for a tumor model with a necrotic core. *J. Sci. Comput.*, 53(2):395–413, 2012.

[34] E.W. Lemmon and M.L. Huber. Thermodynamic properties of n-dodecane. *Energy & Fuels*, 18(4):960–967, 2004.

[35] P. Colonna, N.R. Nannan, A. Guardone, and E.W. Lemmon. Multiparameter equations of state for selected siloxanes. *Fluid Phase Equilibria*, 244(2):193 – 211, 2006.

[36] E.C. Ihmels and E.W. Lemmon. Experimental densities, vapor pressures, and critical point, and a fundamental equation of state for dimethyl ether. *Fluid Phase Equilibria*, 260(1):36 – 48, 2007. Jurgen Gmehling Honour Issue.

[37] M. Richter, M.O. McLinden, and E.W. Lemmon. Thermodynamic properties of 2,3,3,3-tetrafluoroprop-1-ene (r1234yf): Vapor pressure and pt measurements and an equation of state. *Journal of Chemical & Engineering Data*, 56(7):3254–3264, 2011.

[38] R. Akasaka. New fundamental equations of state with a common functional form for 2,3,3,3-tetrafluoropropene (r-1234yf) and trans-1,3,3,3-tetrafluoropropene (r-1234ze(e)). *International Journal of Thermophysics*, 32(6):1125–1147, 2011.